

Dual Halos and Formation of Early-Type Galaxies

Hong Soo PARK¹ & Myung Gyoon LEE¹

hspark@astro.snu.ac.kr & mglee@astro.snu.ac.kr

ABSTRACT

We present a determination of the two-dimensional shape parameters of the blue and red globular cluster systems (GCSs) in a large number of elliptical galaxies and lenticular galaxies (early-type galaxies, called ETGs). We use a homogeneous data set of the globular clusters in 23 ETGs obtained from the HST/ACS Virgo Cluster Survey. The position angles of both blue and red GCSs show a correlation with those of the stellar light distribution, showing that the major axes of the GCSs are well aligned with those of their host galaxies. However, the shapes of the red GCSs show a tight correlation with the stellar light distribution as well as with the rotation property of their host galaxies, while the shapes of the blue GCSs do much less. These provide clear geometric evidence that the origins of the blue and red globular clusters are distinct and that ETGs may have dual halos: a blue (metal-poor) halo and a red (metal-rich) halo. These two halos show significant differences in metallicity, structure, and kinematics, indicating that they are formed in two distinguishable ways. The red halos might have formed via dissipational processes with rotation, while the blue halos are through accretion.

Subject headings: galaxies: elliptical and lenticular, cD — galaxies: formation — galaxies: halos — galaxies: star clusters: general — galaxies: structure

1. Introduction

Early-type galaxies (ETGs, elliptical galaxies and lenticular galaxies) appear to be morphologically simple in their images. However recent accumulating evidence shows that they are more complex and intriguing than ever (Ferrarese et al. 2006; Kormendy et al. 2009; Lee et al. 2010a,b; Zhu et al. 2010; Cappellari et al. 2011; Greene et al. 2012). One of the most surprising and intriguing findings in extragalactic studies during the last two

¹Astronomy Program, Department of Physics and Astronomy, Seoul National University, Korea

decades is a discovery that the color distribution of the globular clusters (GCs) in ETGs is bimodal, suggesting that there are two subpopulations: blue and red GCs (Zepf & Ashman 1993; Geisler et al. 1996; Brodie & Strader 2006; Peng et al. 2008). Blue and red GCs are generally considered to correspond to metal-poor and metal-rich GCs, respectively.

Numerous studies based on observations and simulations followed to investigate the nature and origin of these blue and red subpopulations in ETGs (Brodie & Strader (2006) and references therein). One of the important results is that these subpopulations show differences in one-dimensional spatial distribution: the radial number density profiles of the blue GCs are flatter than those of the red GCs (Kissler-Patig et al. 1997; Lee et al. 1998; Rhode & Zepf 2004; Strader et al. 2011; Forbes et al. 2012). On the other hand, it was suggested that the bimodal color distribution of the GCs can be explained by non-linear transformation between color and metallicity, implying that it is not necessary to believe in the existence of two chemically distinct subpopulations in ETGs (Yoon et al. 2006). Recently several efforts were made to resolve this issue using spectroscopy and near-infrared photometry, but their conclusions are controversial (Woodley et al. 2010; Yoon et al. 2011; Blakeslee et al. 2012; Park et al. 2012; Brodie et al. 2012; Pota et al. 2013).

Two-dimensional spatial distributions of these subpopulations can provide critical clues to settle the controversy of their origin. However, two-dimensional spatial distributions of these subpopulations in the literature show contradictory results. Several studies found that the ellipticity and position angle of both subpopulations are similar to those of the spheroids of their parent galaxies (Forte et al. 2001; Gómez & Richtler 2004; Dirsch et al. 2005; Richtler et al. 2012). On the other hand, other studies presented evidence that the red GCs follow the galaxy ellipticity more closely than the blue GCs (Kissler-Patig et al. 1997; Lee et al. 1998; Forbes et al. 2001; Lee et al. 2008; Strader et al. 2011; Park 2012). It is not yet known whether there is any common feature in the two-dimensional spatial distribution of the GCs among galaxies. One of the best ways to resolve this controversy is to use the structural shapes of the GC systems (GCSs) in a large sample of galaxies, but there has been no such studies to date. In this paper we study the two-dimensional spatial distribution of the blue and red GCs in a large number of ETGs using a homogeneous data set from the Advanced Camera for Surveys Virgo Cluster Survey (ACSVCS) obtained with the Hubble Space Telescope (HST) (Côté et al. 2004; Ferrarese et al. 2006; Jordán et al. 2009).

2. Data and Method

We used data for the position and photometry of the GCs in bright ETGs of the Virgo cluster given in the ACSVCS (Jordán et al. 2009). ACSVCS is a homogeneous gz imaging survey of a sample of 100 ETGs in Virgo with the HST (Côté et al. 2004; Ferrarese et al. 2006). It provided the most comprehensive and homogeneous photometric results on GCs in Virgo so that it is an excellent data set for investigating the properties of GCSs in Virgo galaxies. We selected 23 bright ETGs (including Es, E/S0s, and S0s) in the ACSVCS for our analysis. The numbers of the red GCs are mostly smaller than those of the blue GCs in each galaxy. Therefore we used only the galaxies with a large number of known red GCs ($N \geq 24$). We use the basic properties of the sample galaxies V -band total magnitudes (M_V) from Peng et al. (2008), effective radii (R_e), position angles (P.A.), and ellipticities (ϵ) from Ferrarese et al. (2006), and rotational parameters (λ_{Re}) from Emsellem et al. (2011). We adopted ellipticity and P.A. of each galaxy that are average values measured between $1''$ and effective radius in the g band, although ETGs often show isophotal twisting (Ferrarese et al. 2006). λ_{Re} is a parameter for specific angular momentum (angular momentum normalized to the mass) measured from the stars at the effective radius of the galaxy. It is a sensitive rotation indicator similar to the classical parameter, the ratio between rotational velocity and velocity dispersion (V/σ_v).

To determine two-dimensional shape parameters of the GCSs in each galaxy, we selected first the bright objects with $g_0 < 25.0$ mag and GC probability $P_{GC} > 0.5$ in the ACSVCS GC catalog (Jordán et al. 2009). Next we divided the GC sample into two groups according to their color: the blue GCs ($(g - z)_0 < 1.1$) and the red GCs ($(g - z)_0 > 1.1$).

We investigated two-dimensional shapes of the GCSs in the sample galaxies projected in the sky from the spatial distribution of the GCs. The two-dimensional shapes of the GCSs projected in the images can be approximated with an ellipse. We determined the shape parameters (ellipticity and position angle) of an ellipse for the GCSs in a galaxy, using the method of the dispersion ellipse of the bivariate normal frequency function of position vectors (Trumpler & Weaver 1953). The dispersion ellipse represents a contour at which the density is 0.61 times the maximum density in the center. This method has been often used to estimate the two-dimensional shapes of galaxy clusters or GCSs in a galaxy from a catalog of sources (Carter & Metcalfe 1980; McLaughlin et al. 1994; Hwang & Lee 2007; Strader et al. 2011). We derived the errors for the parameters as 68% confidence levels obtained from the bootstrapping procedure with 1000 trial. We derived the shape parameters for three groups in each galaxy: the entire GCS, the blue GCS, and the red GCS.

Figure 1 displays an example of our shape parameter determination for the blue and red

GCSs in an elliptical (E5) galaxy: M59. In Figure 1(a) the color-magnitude diagram of the GCSs in M59 as well as all other galaxies in the sample shows that the GCSs are divided into two subpopulations: blue and red. In Figure 1(b) and (c) it is seen clearly that the blue GCSs are rather spread over the region, while the red GCSs show a significant central concentration elongated along the major axis of their host galaxy. The ellipticity of the blue GCS we derived is $\epsilon = 0.11 \pm 0.07$, two times smaller than that of the red GCS, $\epsilon = 0.23 \pm 0.07$. The ellipticity of the red GCS is closer to that of the stellar light distribution ($\epsilon = 0.34 \pm 0.02$) than that of the blue GCS. The position angles of the blue and red GCSs are consistent with those of their host galaxies. This shows that there are clear differences in the two-dimensional distribution between the blue and red GCSs in this galaxy, and that our determination of the shape parameters is consistent with visual estimation.

3. Results

Table 1 lists the shape parameters (major axis length, minor axis length, position angle, and ellipticity) derived for the entire GCSs, the blue GCSs, and the red GCSs in 23 ETGs. A comparison of the position angles of the GCSs and those of the stellar light distribution in their host galaxies is displayed in Figure 2. The position angles of the entire, blue, and red GCSs show a good correlation with those of the stellar light distribution for the elongated galaxies with $\epsilon > 0.3$, suggesting that the major axes of the GCSs are well aligned with those of their host galaxies. The large scatter in the position angle differences for less elongated galaxies with $\epsilon < 0.3$ is due to the difficulty in determining the position angles for small ellipticity. This result is consistent with the results in Wang et al. (2013). Using the same data as in this study, Wang et al. (2013) studied the azimuthal variation of the number density of the red and blue GCSs, and found that both systems show alignment with the major axis of their host galaxies.

Figure 3 displays a comparison of the ellipticities of the GCSs we derived and those of the stellar light distribution. The ellipticity of the entire GCSs ($\epsilon(\text{GCS})$) in Figure 3(a) shows a weak correlation with that of the stellar light distribution ($\epsilon(\text{star})$). Linear fits yield $\epsilon(\text{GCS}) = 0.523(\pm 0.108)\epsilon(\text{star}) + 0.016(\pm 0.033)$ and $\text{rms}=0.069$. If we examine the subpopulations separately, the blue GCSs and the red GCSs show a stark contrast with respect to the stellar light distribution (Figure 3(b) and (c)). The ellipticity of the red GCSs shows a strong correlation with that of the stellar light distribution, while the ellipticity of the blue GCSs shows a much weaker correlation (Spearman correlation coefficients are 0.87 for the red GCSs and 0.56 for the blue GCSs). We derive from linear fits, $\epsilon(\text{BGCS}) = 0.342(\pm 0.116)\epsilon(\text{star}) + 0.046(\pm 0.036)$ and $\text{rms}=0.074$ for the blue GCSs, and $\epsilon(\text{RGCS}) =$

$0.959(\pm 0.126)\epsilon(\text{star}) - 0.014(\pm 0.039)$ and $\text{rms}=0.080$ for the red GCSs. Thus the slope for the red GCSs is close to one, while that for the blue GCSs is much smaller than one. These results show that the spatial distributions of the red GCs follow closely those of the stars in their host galaxies, while those of the blue GCs do much less.

Figure 4(a), (b), (e), and (f) display the ellipticity of the blue GCSs, the red GCSs, and the stellar light distribution, as a function of the V -band total magnitude (M_V) of their host galaxies. The ellipticity of the blue GCSs changes little depending on the total magnitude. In contrast, the ellipticity of the red GCSs increases, on average, as their host galaxies get fainter. In Figure 4(e) and (f) linear fits for the ellipticity differences yield $\Delta\epsilon(\text{BGCS} - \text{star}) = -0.045(\pm 0.017)M_V - 1.079(\pm 0.365)$ with $\text{rms}=0.102$, and $\Delta\epsilon(\text{RGCS} - \text{star}) = 0.014(\pm 0.013)M_V + 0.260(\pm 0.280)$ with $\text{rms}=0.079$. The ellipticity differences between the red GCS and stellar light distribution are fit by a linear relation with an almost zero slope, while those between the blue GCS and stellar light distribution are fit by a linear relation with a large slope. This shows that the ellipticities of the red GCSs follow tightly those of the stellar light distribution, irrespective of the luminosity of their host galaxies.

We investigate the relation between the ellipticity of the GCSs and the rotational parameter of their host galaxies (λ_{Re}) (Cappellari et al. 2011; Emsellem et al. 2011) in Figure 4(c), (d), (g), and (h). Figure 4(c) and (d) show that the ellipticity of the red GCSs shows a strong correlation with λ_{Re} , while that of the blue GCSs does not (Spearman correlation coefficient for the red GCSs is 0.80, two times larger than that for the blue GCSs, 0.37). Linear fits for the ellipticity differences in Figure 4(g) and (h) yield $\Delta\epsilon(\text{BGCS} - \text{star}) = -0.204(\pm 0.094)\lambda_{Re} - 0.050(\pm 0.038)$ with $\text{rms}=0.97$, and $\Delta\epsilon(\text{RGCS} - \text{star}) = 0.080(\pm 0.079)\lambda_{Re} - 0.055(\pm 0.032)$ with $\text{rms}=0.081$. The ellipticity differences between the red GCS and stellar light distribution are fit by a linear relation with an almost zero slope, while those between the blue GCS and stellar light distribution are fit by a linear relation with a large slope. This result suggests that the red GCSs may follow closely the kinematics of the stars, irrespective of the rotation parameters of their host galaxies, while the blue GCSs do not. This is consistent with the result that the velocity dispersion and rotation of the red GCSs shows a stronger correlation with that of the stellar light than that of the blue GCSs in several ETGs (Lee et al. 2010b; Pota et al. 2013).

We checked the variation of the ellipticity differences between GCSs and stellar light distribution depending on the color range of GCs using only 13 galaxies with a large number of GCs ($N \geq 24$ in each color bin). We calculated the mean values of the ellipticity differences in the moving color bins with width of $(g - z)_0 = 0.3$ and step of $(g - z)_0 = 0.05$. The mean values of the ellipticity differences are constant at $\Delta\epsilon \sim -0.1$ for $(g - z)_0 = 0.8$

to 1.1, increase to $\Delta\epsilon \sim 0.0$ at $(g - z)_0 \approx 1.4$, and become constant again thereafter. Thus the ellipticity differences between GCSs and stellar light distribution show a hint for discontinuity, indicating that the blue and red GCSs are two distinct components.

4. Discussion

4.1. Dual Halos in ETGs

The differences in the shapes of the blue and red GCSs found in this study show that the origin of the red GCs in ETGs is similar to that of the stars, but different from that of the blue GCs. This indicates that they may represent two separate components in the structure of each galaxy. It is also supported by the fact that the radial number density profiles of the GCs in ETGs show two separate components (e.g., Lee et al. (1998); Forbes et al. (2012)). From these we conclude that there may be dual halos in these galaxies: a blue (metal-poor) halo and a red (metal-rich) halo, in contrast to the traditional view that typical ETGs consist of a single spheroidal component (a single halo). These two halos have significant differences in several aspects. The red halos include red GCs as well as red (metal-rich) stars contributing significantly to the luminosity of their host galaxies, while the blue halos include blue GCs and blue (metal-poor) stars that are barely visible in typical optical images of ETGs because of their low number density (Harris et al. 2007). Typical optical and infrared images of ETGs show only the red halos. The blue halos are metal-poor, while the red halos are metal-rich. The red halos are spatially more elongated and centrally concentrated than the blue halos. The blue halos are much more extended than the red halos, as seen in the GC map of the Virgo cluster (Lee et al. 2010a). The red halos may be rotating, while the blue halos do little (Lee et al. 2010b; Pota et al. 2013). It is noted that the dual nature of the GCSs in ETGs is similar to that of the dual stellar halos in the Milky Way Galaxy (Carollo et al. 2007; Beers et al. 2012; McCarthy et al. 2012).

The similarity in the shapes of the red GCSs and the stellar light distribution implies also that the red GCSs and stars may share their history from their birth in ETGs. In addition, the radial color profiles of the red GCs in ETGs are known to be similar to those of the stellar light (Lee et al. 1998; Brodie & Strader 2006; Richtler et al. 2012; Park 2012). These results suggest that the red GCs and stars in ETGs are formed in the same place and follow similar dynamical evolution. The large range of their ellipticity indicates that the ETGs have a diverse rotational property, consistent with the results from stellar kinematics (Cappellari et al. 2011; Emsellem et al. 2011). These also suggest that the red halos might have formed mostly via various gaseous mergers (Khochfar et al. 2011) and/or dissipative collapse of the rotating proto-disks (McCarthy et al. 2012). The fact that the red GCSs

have on average higher values of ellipticity than the blue GCSs indicates that the red halos might have been involved with major gaseous mergers in the later epochs than the blue halos.

On the other hand, the small ellipticity and blue color of the blue GCSs and their independence from stellar light distribution show that they were formed separately from stars in the main body of ETGs. The blue GCs might have formed mostly in low-mass dwarf galaxies and they were accreted later to their current host galaxies via mass assembly during the growing phase of ETGs (Côté et al. 1998, 2000; Brodie & Strader 2006; Lee et al. 2010b; Park et al. 2012; Tonini 2013). Independence of the ellipticity of the blue GCSs from the luminosity of their host galaxies indicates that their formation mechanism may not depend much on the galaxy mass.

The formation history of these two halos is consistent with the two-phase models for galaxy formation based on numerical simulations (Oser et al. 2010). Previous simulations on ETGs are focused on explaining mostly the stellar light distribution in ETGs. However, future simulations need to include both the blue and red GCSs as well as the stellar light distribution for better understanding how ETGs formed. Our results on the difference in the two-dimensional shapes of the blue GCSs and the red GCSs in ETGs, as well as kinematics of GCSs in ETGs (Lee et al. 2010b; Pota et al. 2013) and bimodal metallicity distributions of GCs in some ETGs (Woodley et al. 2010; Park et al. 2012; Brodie et al. 2012), are against the scenario suggested by Yoon et al. (2006, 2011) that ETGs do not have to possess two distinct sub-populations of GCs.

4.2. Shapes of the Stellar Halos in ETGs

We checked the ratio of the ellipticity of the blue and the red GCSs to the ellipticity of the stellar light distribution as a function of major axis length of the GCSs ($a(\text{GCS})$) divided by effective radii of their host galaxies (R_e). The values of $a(\text{GCS})/R_e$ indicate the relative sizes of the measured GCSs with respect to the sizes of the stellar light distribution of their host galaxies. The ellipticity ratios of the blue and red GCSs vary little depending on $a(\text{GCS})/R_e$. The mean value of the ratio for the blue GCS is $\epsilon(\text{BGCS})/\epsilon(\text{star}) = 0.51 \pm 0.30$, which is much smaller than that for the red GCS (0.95 ± 0.41). This result shows that the two-dimensional shapes of the blue GCSs are rounder than those of the red GCSs regardless of galactocentric radius. If the kinematics of the blue GCSs in the outer region of their host galaxy are combined with the shapes of the GCSs, it will provide a strong constraint to study the distribution and shapes of the dark matter halos (Sackett 1999; Mo et al. 2010).

Previous studies found evidence for the existence of metal-poor halo stars as well as metal-rich halo stars in some ETGs. Harris et al. (2007) found, from the deep photometry of the halo stars in a remote field located at 33 kpc from the center of NGC 3379 (E1), that the metallicity distribution of the stars is extremely broad and flat, requiring a need for a distinct two-stage chemical evolution model. From this they also predicted that most large ETGs will host diffuse, very low-metallicity halo components. However, their field covered only a tiny fraction of the halo so that their results could not tell about the geometric shape of the halo. Our results suggest that the metal-poor halo in this galaxy is less elongated than the red halo.

The authors are grateful to Prof. Paul Hodge, and Drs. Ho Seong Hwang and Narae Hwang for reading carefully the original manuscript and their useful comments. This work was supported by the National Research Foundation of Korea (NRF) grant funded by the Korea Government (MEST) (No.2013R1A2A2A05005120).

REFERENCES

- Beers, T., et al., 2012, *ApJ*, 746, 34
- Blakeslee, J. P., et al., 2012, *ApJ*, 746, 88
- Brodie, J. P., & Strader, J., 2006, *ARA&A*, 44, 193
- Brodie, J. P., et al., 2012, *ApJ*, 759, L33
- Cappellari, M. et al. 2011, *MNRAS*, 416, 1680
- Carollo, D., et al., 2007, *Nature*, 450, 1020
- Carter, D., & Metcalfe, N., 1980, *MNRAS*, 191, 325
- Côté, P., Marzke, R. O., West, M. J. 1998, *ApJ*, 501, 554
- Côté, P., Marzke, R. O., West, M. J., Minniti, D. 2000, *ApJ*, 533, 869
- Côté, P., et al., 2004, *ApJS*, 153, 223
- Dirsch, B., Schubert, Y., & Richtler, T., 2005, *A&A*, 433, 43
- Emsellem, E., et al., 2011, *MNRAS*, 414, 888
- Ferrarese, L., et al., 2006, *ApJS*, 164, 334

- Forbes, D. A., Ponman, T., & O’Sullivan, E., 2012, MNRAS, 425, 66
- Forbes, D. A., Georgakakis, A. E., & Brodie, J. P., 2001, MNRAS, 325, 1431
- Forte, J. C., et al. 2001, AJ, 121, 1992
- Geisler, D., Lee, M. G., & Kim, E. 1996, AJ, 111, 1529
- Gómez, M., & Richtler, T., 2004, A&A, 415, 499
- Greene, J. E. et al. 2012, ApJ, 750, 32
- Harris, W. E., Harris, G. L. H., Layden, A. C., & Wehner, E. M. H., 2007, ApJ, 666, 903
- Hwang, H. S., & Lee, M. G., 2007, ApJ, 662, 236
- Jordán, A., et al., 2009, ApJS, 180, 54
- Khochfar, S., et al., 2011, MNRAS, 417, 845
- Kissler-Patig, M., Richtler, T., Storm, J., & della Valle, M., 1997, A&A, 327, 503
- Kormendy, J., Fisher, D. B., Cornell, M. E., & Bender, R. 2009, ApJS, 182, 216
- Lee, M. G., Park, H. S., & Hwang, H. S., 2010a, Science, 328, 334
- Lee, M. G., Park, H.S., Hwang, H. S., et al., 2010b, ApJ, 709, 1083
- Lee, M. G., Park, H.S., Kim, E., et al., 2008, ApJ, 682, 135
- Lee, M. G., Kim, E., & Geisler, D., 1998, AJ, 115, 947
- McCarthy, I. G., et al., 2012, MNRAS, 420, 2245
- McLaughlin, D. E., Harris, W. E., & Hanes, D. A., 1994, ApJ, 422, 486
- Mo, H., van den Bosch, F. C., & White, S., 2010, Galaxy Formation and Evolution, Cambridge, Chap. 7
- Oser, L., et al., 2010, ApJ, 725, 2312
- Park, H. S., Lee, M. G., Hwang, H. S., et al., 2012, ApJ, 759, 116
- Park, H. S., 2012, Jour. Korean Astron. Soc., 45, 71
- Peng, E. W., et al., 2008, ApJ, 681, 197

- Pota, V. et al., 2013, MNRAS, 428, 389
- Richtler, T., Bassino, L. P., Dirsch, B., & Kumar, B., 2012, A&A, 543, 131
- Rhode, K. L. & Zepf, S. E. 2004, AJ, 127, 302
- Sackett, P. 1999, in ASP Conf. Ser. 182, Galaxy Dynamics, ed. D. R. Merritt, M. Valluri, & J. A. Sellwood (San Francisco: ASP), 393
- Strader, J., et al., 2011, ApJS, 197, 33
- Tonini, C. 2013, ApJ, 762, 39
- Trumpler, R. J., & Weaver, H. F., 1953, Statistical Astronomy (Univ. California Press), Berkeley
- Wang, Q., et al., 2013, ApJ, 769, 145
- Woodley, K. A., et al., 2010, ApJ, 708, 1335
- Yoon, S.-J., Yi, S. K., & Lee, Y.-W., 2006, Science, 311, 1129
- Yoon, S.-J., et al., 2011, ApJ, 743, 149
- Zepf, S. E., & Ashman, K. M., 1993, MNRAS, 264, 611
- Zhu, G., Blantod, M. R., & Moustakas, J. 2010, ApJ, 722, 491

Table 1. Shape parameters for the GCSs in the 23 galaxies

VCC	$N(\text{GC})$	a (arcsec)	b (arcsec)	P.A. (deg)	ϵ
<u>Entire GCSs</u>					
1226	635	54.2 ± 1.1	50.8 ± 1.0	93.6 ± 15.3	0.062 ± 0.028
1316	1468	52.1 ± 0.7	50.0 ± 0.7	80.5 ± 17.8	0.040 ± 0.019
1978	670	52.5 ± 1.3	45.0 ± 1.1	82.2 ± 05.7	0.144 ± 0.033
1903	280	50.6 ± 2.0	41.3 ± 1.8	162.7 ± 07.1	0.183 ± 0.052
....					
<u>Blue GCSs</u>					
1226	232	55.3 ± 1.8	50.6 ± 1.8	101.1 ± 21.1	0.086 ± 0.043
1316	530	55.0 ± 1.1	50.9 ± 1.1	88.1 ± 15.2	0.076 ± 0.027
1978	234	52.1 ± 1.7	48.5 ± 1.5	54.7 ± 23.7	0.071 ± 0.045
1903	108	51.0 ± 2.6	45.2 ± 2.5	161.2 ± 22.0	0.112 ± 0.069
....					
<u>Red GCSs</u>					
1226	403	53.6 ± 1.3	50.9 ± 1.2	86.7 ± 26.0	0.050 ± 0.034
1316	938	50.4 ± 0.8	49.3 ± 0.9	63.2 ± 35.8	0.022 ± 0.021
1978	436	53.2 ± 1.5	42.3 ± 1.3	87.1 ± 05.0	0.205 ± 0.036
1903	172	50.1 ± 2.6	38.5 ± 2.4	164.4 ± 07.2	0.232 ± 0.065
....					

Note. — This table is available in the online journal.

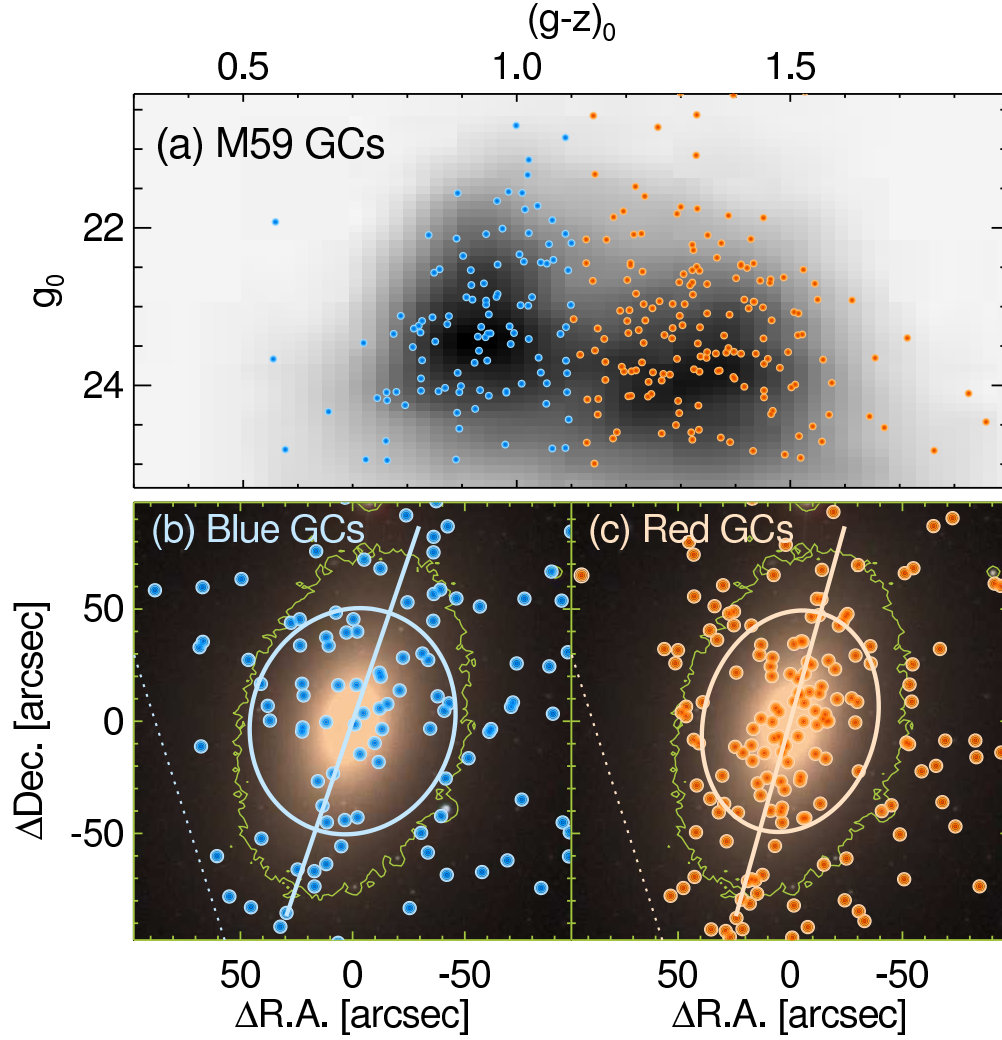


Fig. 1.— An example for deriving the shape parameters of the GCSs in a galaxy: M59 (VCC 1903), an E5 galaxy. (a) The color-magnitude diagram for blue and red GCs in M59. The grey-scale image represents the number density map of the GCs in all 23 galaxies. (b) and (c) Spatial distributions of the blue and red GCs, respectively. The solid ellipses and lines represent the shapes and position angles determined for the GCSs, respectively. Green contours represent reference isophote contours overlaid on Sloan Digital Sky Survey color images for M59. Dotted lines represent the boundary of the HST images.

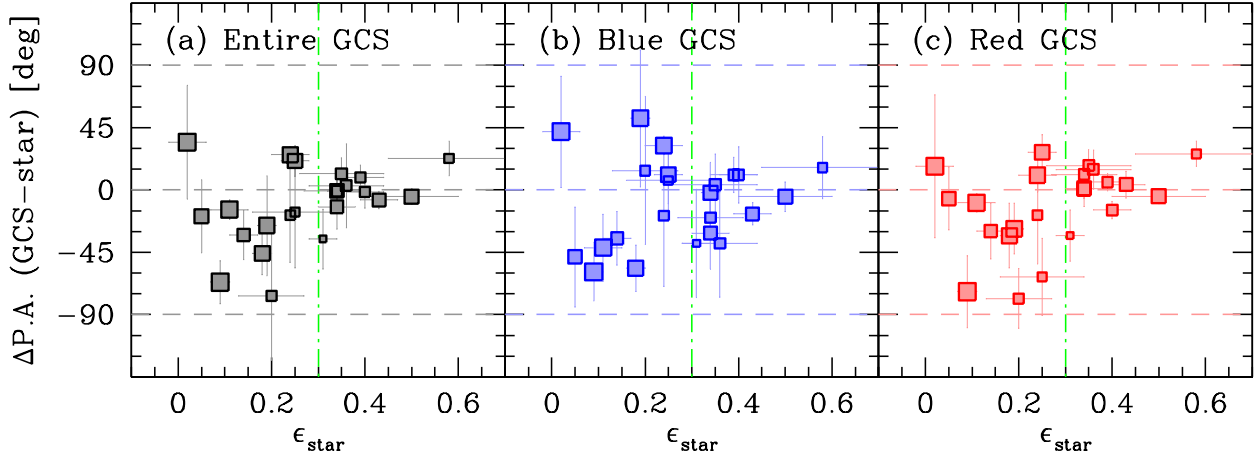


Fig. 2.— Position angle differences (Δ P.A.) of the entire GCSs (a), the blue GCSs (b), and the red GCSs (c) with respect to their host galaxies versus ellipticities of the stellar light distribution (ϵ_{star}). The dot-dashed lines represent $\epsilon_{\text{star}} = 0.3$. Symbol sizes represent the relative brightness of the host galaxies: the larger, the brighter.

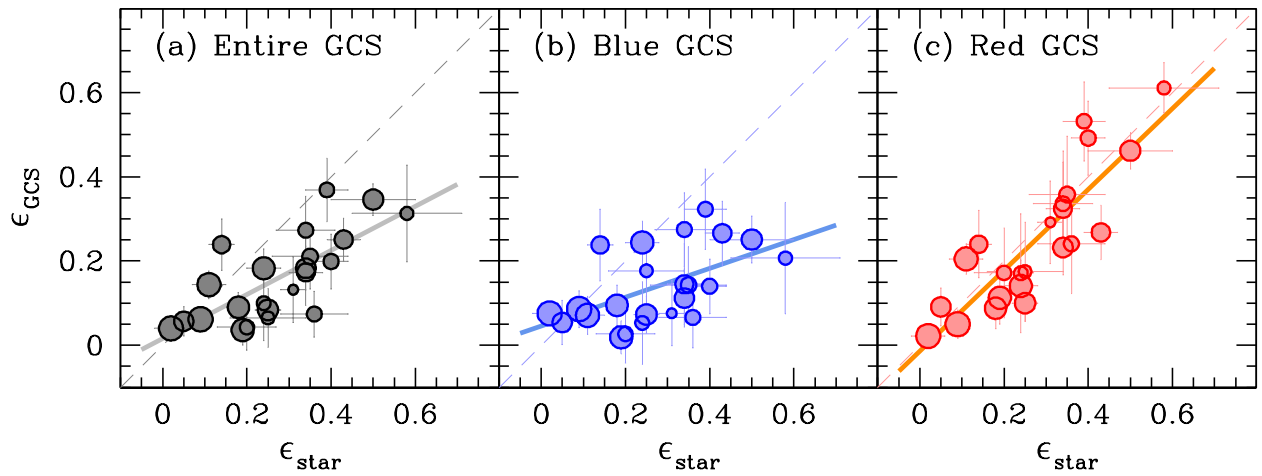


Fig. 3.— Ellipticities of the GCSs versus those of stellar light distribution in their host galaxies. (a) the entire GCSs, (b) the blue GCSs, and (c) the red GCSs. Symbol sizes are same as Figure 2. The dashed lines represent one-to-one relations, and the solid lines represent linear fits.

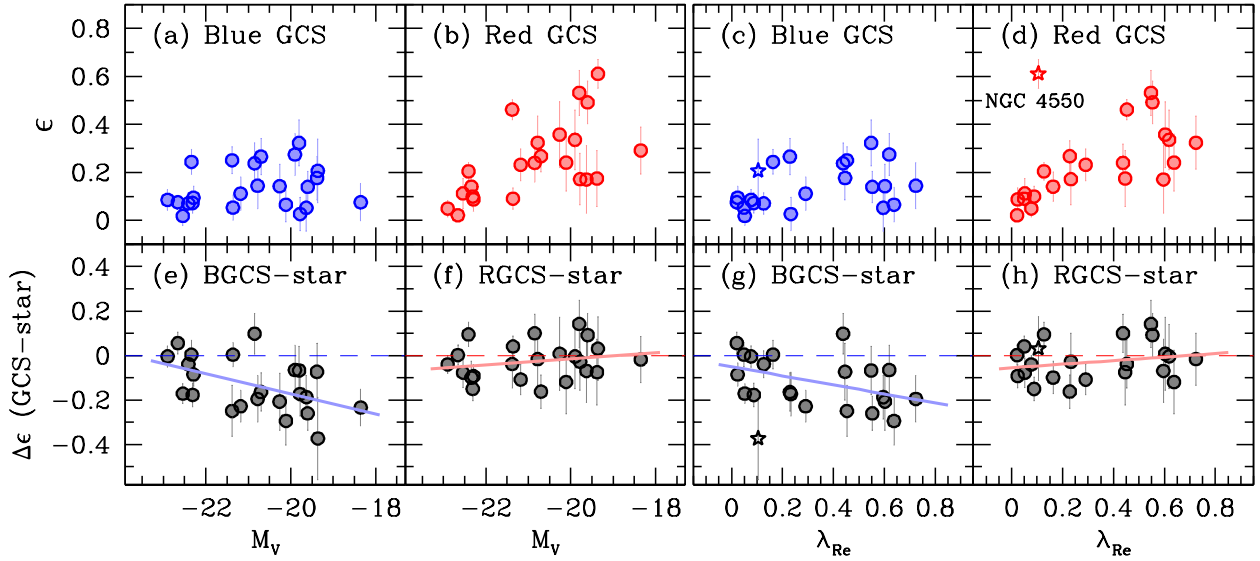


Fig. 4.— Ellipticities (ϵ) of the GCSs versus V -band total magnitudes (M_V) and rotation parameters (λ_{Re}) of their host galaxies. (a), (b) Ellipticities of the blue and red GCSs versus M_V . (c), (d) Ellipticities of the blue and red GCSs versus λ_{Re} . (e), (f) Ellipticity differences between the GCSs and stellar light distributions versus M_V for the blue and red GCSs, respectively. Solid lines represent linear fits. (g), (h) Ellipticity differences between the GCSs and stellar light distributions versus λ_{Re} for the blue and red GCSs, respectively. One outlier with a large ellipticity and small λ_{Re} (open starlet) is NGC 4550 (VCC 1619). It is a highly elongated (E7/S0) galaxy, but is known to have counter-rotating components resulting in low rotation (Emsellem et al. 2011).